Light-Operated Machines Based on Threaded Molecular Structures

Alberto Credi, Serena Silvi, and Margherita Venturi

Abstract Rotaxanes and related species represent the most common implementation of the concept of artificial molecular machines, because the supramolecular nature of the interactions between the components and their interlocked architecture allow a precise control on the position and movement of the molecular units. The use of light to power artificial molecular machines is particularly valuable because it can play the dual role of "writing" and "reading" the system. Moreover, light-driven machines can operate without accumulation of waste products, and photons are the ideal inputs to enable autonomous operation mechanisms. In appropriately designed molecular machines, light can be used to control not only the stability of the system, which affects the relative position of the molecular components but also the kinetics of the mechanical processes, thereby enabling control on the direction of the movements. This step forward is necessary in order to make a leap from molecular machines to molecular motors.

Keywords Molecular machines · Molecular memories · Photochemistry · Rotaxanes · Unidirectional motion

Contents

A. Credi (✉), S. Silvi, and M. Venturi
Dipartimento di Chimica "G. Ciamician", Università di Bologna, and Interuniversity Center for the Chemical Conversion of Solar Energy (SolarChem), Via Selmi, 2, 40126 Bologna, Italy
e-mail: alberto.credi@unibo.it

Abbreviations

bpy	2,2'-Bipyridine
BPY^{2+}	4,4'-Bipyridinium
$CBPQT^{4+}$	Cyclobis(paraquat-*p*-phenylene)
α-CD	α-Cyclodextrin
CT	Charge-transfer
DBA^+	Dibenzylammonium
DNP	1,5-Dioxynaphthalene
MBA^+	Monobenzylammonium
NMR	Nuclear magnetic resonance
^{t}Bu	*tert*-Butyl
TMeAB	3,5,3',5'-Tetramethylazobenzene
TTF	Tetrathiafulvalene

1   Introduction

The interaction between light and matter lies at the heart of the most important processes of life [1]. Light consists of photons which are exploited by natural systems as both quanta of energy and elements of information. All the natural phenomena related to the interaction between light and matter and the great number of applications of photochemistry in science and technology can ultimately be traced back to these two aspects of light. Living examples of this double-faced nature of light are provided by the two most important photochemical processes taking place in the biological world: photosynthesis and vision.

A variety of functions can also be obtained from the interaction between light and matter in artificial systems [2]. The type and utility of such functions depend on the degree of complexity and organization of the chemical systems that receive and process the photons. Indeed, understanding the interaction between light and molecules, together with the progress in chemical synthesis, has led to the point where one can conceive and assemble artificial multicomponent systems capable of using light as an energy supply and/or as an input signal. The construction of such

ultraminiaturized devices and the comprehension of their working mechanisms are based on the concepts of supramolecular chemistry [3] and photochemistry [4], and have become topics of great interest for nanoscience.

In general terms, a molecular machine can be defined [5, 6] as an assembly of a discrete number of molecular components designed to perform specific mechanical movements in response to appropriate external stimuli. The nanomachines of the biological world [7, 8], such as ATPase and myosin, are the premier, proven examples of the feasibility and utility of nanotechnology [9], and constitute a sound rationale for attempting the realization of artificial molecular machines. As the bottom-up construction of devices of such a complexity is currently a prohibitive task, chemists have been trying to make much simpler systems, to understand the principles and processes at the basis of their operation, and to investigate the problems posed by interfacing them with the macroscopic world.

The photochemical tweezers described [10] by Shinkai and coworkers in the early 1980s can be considered as primitive examples of molecular machines; in fact, systems of this type have evolved to a considerable degree of complexity [11]. The concept of artificial photochemically driven molecular machine, however, was illustrated and realized for the first time in 1993 in a landmark paper by Balzani, Stoddart and coworkers [12]. Since then, the development of powerful synthetic methodologies, combined with a device-driven ingenuity evolved from the attention to functions and reactivity, have led to remarkable achievements. Several reviews [6, 13–18] and a monograph [5] dealing with light-operated molecular machines are available.

In this chapter we discuss the possibilities offered by the use of light to operate molecular machines, namely, to supply energy to the system and/or gain information on its state. After some general considerations, a few recent examples of photochemically controlled molecular machines based on rotaxanes and related compounds, most of them studied in our laboratory, are described. They present some small, although interesting, advancements in exploiting the peculiar properties of light and its interaction with matter to obtain useful functions.

2 The Role of Light

2.1 Energy Supply and Monitoring Signals

As happens in the macroscopic world, molecular-level devices and machines need energy to operate and signals to communicate with the operator [19]. The most obvious way to supply energy to a chemical system is through an exergonic chemical reaction. Not surprisingly, the majority of the molecular motors of the biological world are powered by chemical reactions (e.g., ATP hydrolysis) [7–9]. Richard Feynman observed [20] that "an internal combustion engine of molecular size is impossible. Other chemical reactions, liberating energy when

cold, can be used instead." This is exactly what happens in our body, where the chemical energy supplied by food is used in long series of slightly exergonic reactions to power the biological machinery that sustains life.

If an artificial molecular machine has to work by inputs of chemical energy, it will need addition of fresh reactants ("fuel") at any step of its working cycle, with the concomitant formation of waste products. Accumulation of waste products, however, will compromise the operation of the device unless they are removed from the system, as happens in our body as well as in macroscopic internal combustion engines. The need to remove waste products introduces noticeable limitations in the design and construction of artificial molecular machines based on chemical fuel inputs.

Chemists have long known that photochemical and electrochemical energy inputs can cause the occurrence of *endergonic* and *reversible* reactions. In the last few years the outstanding progress made by supramolecular methodologies [21, 22], in particular photochemistry [23] and electrochemistry [24], has led to the design and construction of molecular machines powered by light or electrical energy which work without formation of waste products.

In the context of artificial nanomachines, light energy stimulation possesses a number of further advantages, particularly in comparison with chemical stimulation. First of all, the amount of energy conferred to a chemical system by using photons can be carefully controlled by the wavelength and intensity of the exciting light, in relation to the absorption spectrum of the targeted species. Such energy can be transmitted to molecules without physically connecting them to the source (no "wiring" is necessary), the only requirement being the transparency of the matrix at the excitation wavelength. Other properties of light, such as polarization, can also be utilized. Lasers provide the opportunity of working in very small spaces and extremely short time domains, and near-field techniques allow excitation with nanometer resolution. On the other hand, the irradiation of large areas and volumes can be conveniently carried out, thereby allowing the parallel (or even synchronous) addressing of a very high number of individual nanodevices.

Because molecules are extremely small, the observation of motion at the molecular level, which is crucial for monitoring the operation of a molecular machine, is not trivial. In general, the motion of the component parts should cause readable changes in some chemical or physical properties of the system. Photochemical methods are also useful in this regard. As a matter of fact, photons can play with respect to chemical systems the dual role of *writing* (i.e., causing a change in the system) and *reading* (i.e., reporting the state of the system) [23]. As discussed in the introduction, this is primarily true in nature, where sunlight photons are employed both as energy quanta in photosynthetic processes, and as information elements in vision and other light-triggered processes. For example, luminescence spectroscopy is a valuable method because it is easily accessible and offers good sensitivity and selectivity, along with the possibility of time- and space-resolved studies [25]. In particular, flash spectroscopic techniques with laser excitation enable the study of extremely fast processes.

The use of light to power nanoscale devices is relevant for another important reason. If and when a nanotechnology-based industry will be developed, its products will have to be powered by renewable energy sources, because it has become clear that the problem of energy supply is a crucial one for human civilization for the years ahead [26]. In this frame, the construction of nanodevices, including natural-artificial hybrids [27] that harness solar energy in the form of visible or near-UV light, is indeed an important possibility.

2.2 Autonomous Operation

An important feature of a molecular machine is its capability to exhibit an autonomous behavior, i.e., to operate without external intervention (in other words, in a constant environment) as long as the energy source is available. Hence, autonomous molecular machines are free-running devices that do not require controlled and repeated addition of chemicals or other environmental changes. Natural motors are autonomous, in most cases acting as catalyzers for the fueling reaction. Except for some work on DNA nanodevices [28, 29], the chemically powered artificial molecular machines reported so far are not autonomous because after the mechanical movement induced by a given input they need another, opposite, input to be reset.

The design of autonomous nanomachines can take advantage from reversible photochemical processes. For instance, the operation of the machine could be based on a photoinduced sequence of processes that lead the system through transient electronic and nuclear (mechanical) states; the final deactivation of the system to the ground state provides an automatic reset and closes the cycle of operation. Alternatively, the mechanical motion could be related to the light-triggered switching between two stable states as happens in photochromic systems. These approaches will be more conveniently discussed in the examples illustrated in Sects. 4 and 5.

3 Threaded and Interlocked Multicomponent Species

In principle, molecular machines can be designed starting from several kinds of molecular and supramolecular systems [5, 6, 13, 30–42], including DNA [43, 44]. However, for the reasons mentioned below, most of the systems constructed so far are based on interlocked molecular species such as rotaxanes and related species. The names of these compounds are derived from the Latin words *rota* and *axis* for wheel and axle, respectively. Rotaxanes [45] are minimally composed (Fig. 1a, b) of a dumbbell-shaped molecule surrounded by a macrocyclic compound (the "ring") and terminated by bulky groups ("stoppers") that prevent disassembly. If the stoppers are not present, the assembled species is denoted as a pseudorotaxane and in solution it equilibrates with the separated axle-type and ring
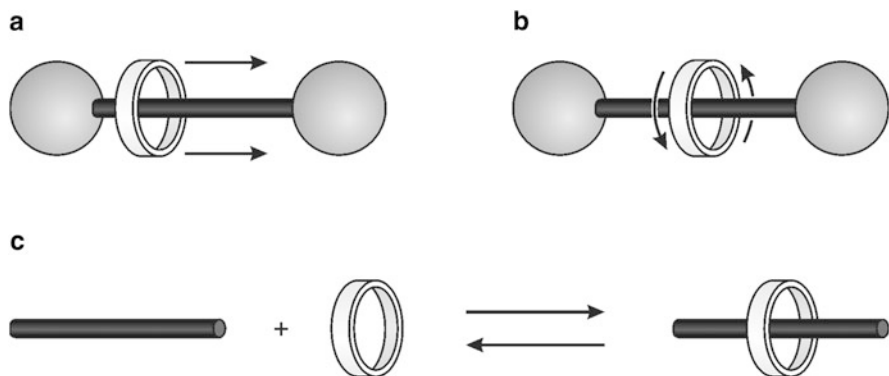
Fig. 1 Schematic representation of (**a**) ring shuttling and (**b**) ring rotation in rotaxanes, and (**c**) the threading/dethreading equilibrium involving the axle-type and ring components of a pseudorotaxane

components (Fig. 1c). Important features of these systems arise from noncovalent interactions between the components that contain complementary recognition sites. Such interactions are responsible for the self-assembly of pseudorotaxanes and efficient template-directed syntheses of rotaxanes, and include electron donor–acceptor ability, hydrogen bonding, hydrophobic–hydrophylic character, π–π stacking, electrostatic forces and, on the side of the strong interaction limit, metal-ligand bonding.

Rotaxanes are appealing systems for the construction of molecular machines because (1) the mechanical bond enables a large variety of mutual arrangements of the molecular components while conferring stability to the system, (2) the interlocked architecture limits the amplitude of the intercomponent motion in the three directions, (3) the stability of a specific arrangement (co-conformation) is determined by the strength of the intercomponent interactions, and (4) such interactions can be modulated by external stimulation. Two interesting molecular motions can be envisaged in rotaxanes, namely *translation*, i.e., shuttling of the ring along the axle (Fig. 1a), and *rotation* of the ring around the axle (Fig. 1b). Hence, rotaxanes are good prototypes for the construction of both linear and rotary molecular machines. Systems of the first type, termed molecular shuttles, constitute the most common implementation of the molecular machine concept with rotaxanes.

The assembly–disassembly of the axle-type and ring components of a pseudorotaxane (Fig. 1c) is reminiscent of the threading/dethreading of a needle and can be controlled by external stimulation [5, 46]. Studies on switchable pseudorotaxanes are important for the development of less trivial unimolecular machines based on rotaxanes and related interlocked compounds.

It should be noted that, unless one of the molecular components of the assembly is attached to a fixed support (e.g., a surface) in a rigid manner, "moving" and "static" parts cannot be meaningfully identified. Hence, for systems working in solution, it is correct to refer to the processes shown in Fig. 1 as *relative* movements of the components with respect to one another.

Moreover, the drawings shown in Fig. 1, while providing a simple structural and topological representation, are somewhat misleading because they give the impression that rotaxanes are made of rigid molecular components, which is not the case for the vast majority of the systems reported so far. However, in order to obtain clear-cut mechanical movements the molecular components should exhibit at least some stiffness. As will be evidenced by the examples in the following sections, this feature for molecular machines is most commonly fulfilled by utilizing molecular components that possess rigid subunits in their structures.

Interestingly, the dumbbell component of a molecular shuttle exerts on the ring motion the same type of directional restriction imposed by the protein track for linear biomolecular motors (an actin filament for myosin and a microtubule for kinesin and dynein) [7]. It should also be noted that interlocked molecular architectures are largely present in natural systems – for instance, DNA catenanes and rotaxanes are known [45]. Many processive enzymes, that is, enzymes that remain attached to their biopolymer substrates (DNA, RNA, or proteins) and perform multiple rounds of catalysis before dissociating, are thought to exhibit a rotaxane structure, as confirmed for example by the observation of the crystal structure of DNA λ-exonuclease ([47] and references therein). Clearly, the unique aspect of the rotaxane architecture, that is, the mechanical binding of the catalyst with the substrate which leaves the former free to displace itself along the latter without losing the system's integrity, is utilized by Nature to enhance the activity of processive enzymes.

4 Molecular Shuttles and Related Systems

Molecular shuttles are rotaxanes in which the ring component can move along the axle portion of the dummbell-shaped component [48]. These types of systems constitute a common implementation of the molecular machine concept with artificial chemical systems [5, 6, 13]. The minimal design for a controllable molecular shuttle [49] involves the incorporation of two different recognition sites (stations) on the axle. The ring originally encircles the most efficient station until a chemical reaction, properly activated, changes the relative affinity between the ring and the stations, thereby causing the translation of the ring to the other station.

Light stimulation of molecular shuttles can have two main effects: (1) modify the interactions of the ring with the stations, i.e., the thermodynamic stability of the mechanical states involved in the operation of the machine, and/or (2) control the transition rates between such states, i.e., the kinetics of the mechanical motions. Photoinduced electron-transfer processes, both intramolecular [50, 51] and intermolecular [52, 53], and photoisomerization reactions [54–58] have been largely employed for purpose (1) above. Photoisomerization processes can also be profitably used for controlling the kinetics of molecular motions (point (2)) [59], as shown in some of the examples reported in the following.
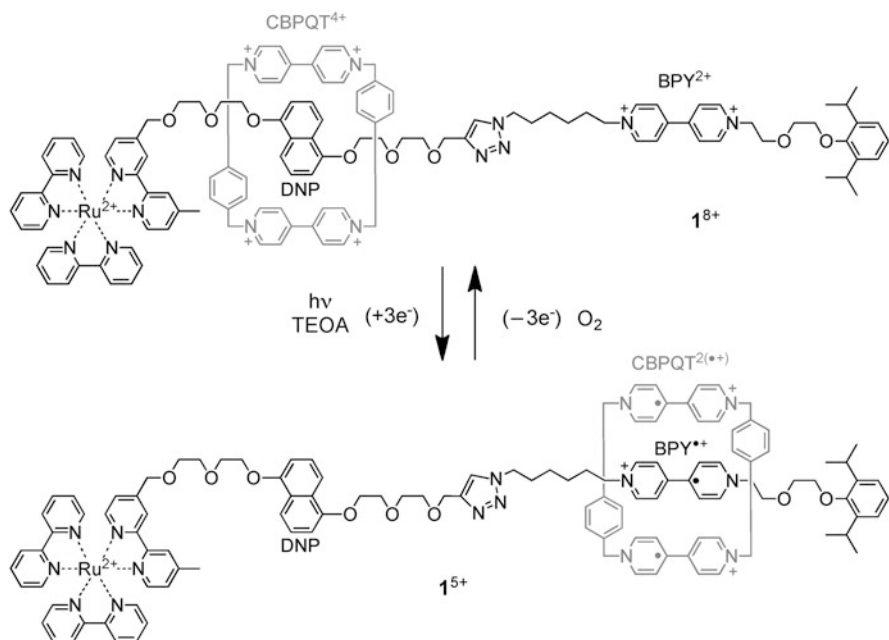
Fig. 2 Structural formula and schematic representation of the light-induced and chemically assisted shuttling movements of bistable rotaxane $\mathbf{1}^{8+}$

4.1 Molecular Shuttling Operated by Photoswitching of Radical–Radical Interactions

An example of a molecular shuttle based on photoinduced electron transfer and exploiting radical–radical interactions in water was recently described [60]. The design of the system relies on previously investigated rotaxanes utilizing ruthenium(II) polypyridine-type complexes as electron-transfer photosensitizers [50, 61, 62]. The investigated rotaxane $\mathbf{1}^{8+}$ (Fig. 2) consists of the electron acceptor macrocycle cyclobis(paraquat-p-phenylene), $CBPQT^{4+}$, and a dumbbell-shaped component that contains four units: (1) a $Ru(bpy)_3^{2+}$-type complex (bpy = 2,2'-bipyridine) which plays the dual role of a photosensitizer and a stopper (Ru^{2+}), (2) a 1,5-dioxynaphthalene electron donor unit (DNP), (3) a 4,4'-bipyridinium electron acceptor site (BPY^{2+}), and (4) a diisopropylbenzene moiety as the second stopper. The behavior of rotaxane $\mathbf{1}^{8+}$ and of its molecular components was investigated by means of NMR and UV-visible spectroscopy, and by electrochemical techniques.

In the starting co-conformation of $\mathbf{1}^{8+}$, the $CBPQT^{4+}$ macrocycle encircles the DNP site on account of π-donor–acceptor interactions (Fig. 2). Irradiation of a deoxygenated water solution of the rotaxane with visible light (absorbed exclusively by the Ru^{2+} unit) causes an electron transfer from the excited state of

Ru^{2+} to the bipyridinium dications present both in the $CBPQT^{4+}$ ring and in the axle (BPY^{2+}). Triethanolamine (TEOA) added at a sufficiently high concentration acts as a sacrificial reductant, thereby preventing the back electron transfer from the bipyridinium radical cations to the oxidized Ru^{3+} center. As a consequence, upon exhaustive irradiation, all three of the bipyridinium units (two in the ring and one in the axle) are converted to the monoreduced forms and are accumulated in the solution. The resulting diradical dicationic $CBPQT^{2(\cdot +)}$ ring undergoes translation in order to encircle the $BPY^{\cdot +}$ unit in the axle, on account of stabilizing radical–radical interactions (signaled by the characteristic absorption bands in the visible region [63, 64]) and the weakening of the π-donor–acceptor interaction between the reduced ring and the DNP donor unit. As soon as the bipyridinium radical cations are oxidized by oxygen, the restoration of the donor–acceptor interactions of $CBPQT^{4+}$ and DNP, together with the increased electrostatic repulsion between $CBPQT^{4+}$ and BPY^{2+}, induces the ring to shuttle back and encircle the DNP unit (Fig. 2).

In principle, the shuttling mechanism of rotaxane $\mathbf{1}^{8+}$ should enable light-powered autonomous operation of the molecular machine, as observed earlier with similar systems [51, 52]. The experiments performed so far, however, do not allow one to gather information in this regard. The investigation of such an important issue would require time-resolved spectroscopic experiments, possibly replacing TEOA with a non-sacrificial reductant as an electron relay capable of electronically resetting the system when ring shuttling has occurred [51, 52].

4.2 Extension-Contraction of a Rotaxane Dimer

An exciting development in the field of artificial molecular machines has been the construction of molecules that can stretch and contract upon external stimulation [65]. Systems of this kind remind the operation of the sarcomere, that is, the basic functional element of skeletal muscles, in which the simultaneous sliding of the stacked filaments of myosin and actin powered by ATP hydrolysis causes a change in the sarcomere length [7, 8]. In a muscle fiber the extension and contraction of a large number of sarcomeres is summed up, causing a macroscopic mechanical effect. Similarly, it can be imagined that polymers obtained from monomers that can perform a reversible change in length (or volume) upon stimulation could enable the amplification of nanoscale motions up to the macroscopic scale, thus obtaining artificial molecule-based muscles [16].

The first attempts to develop artificial molecular muscles was based on the combination of the concept of controllable molecular shuttle [49, 66] with the topology of a rotaxane dimer (Fig. 3) [67]. Rotaxane-based muscles operated by chemical stimulation have been reported [68] and have recently been utilized to make covalent and coordination polymers in which collective extension and contraction effects are obtained [69, 70].

Fig. 3 Schematic representation of the stimuli-induced extension-contraction motion of a bistable rotaxane dimer


Extended

Stimulus   Stimulus

Contracted
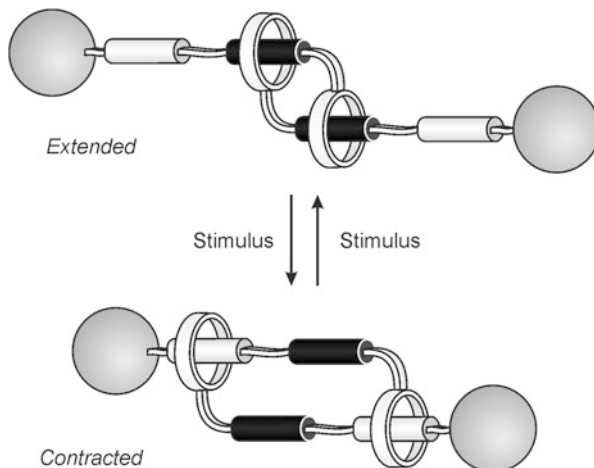
An interesting example of a molecular muscle operated by light is represented by compound **2** shown in Fig. 4 [71]. This rotaxane dimer comprises α-cyclodextrin (α-CD) as the macrocyclic components and photoisomerizable stilbene units in the axle components. It is well known that stilbene in the *E*-configuration is effectively included within α-CD. Indeed, 2D NMR spectroscopy showed that in the *E*, *E* isomer of **2** the stilbene units are surrounded by the α-CD rings. Irradiation of *E,E*-**2** at 350 nm in water afforded a photostationary state composed of the *E,E*-, *E*, *Z*-, and *Z,Z*-isomers of **2** in a ratio of ca. 2:2:1. Subsequent irradiation at 254 nm to target the *Z*-stilbene units yielded a photostationary mixture containing *E,E*- and *E*, *Z*-**2** in a ratio of ca. 6:1. The reversibility of the process was monitored by alternating irradiation at 350 nm and at 254 nm. The photoproducts were isolated by HPLC and subjected to NMR analysis, which showed that in *Z,Z*-**2** the α-CD rings are moved off the *Z*-stilbene moieties towards the propyl and blocking groups. The movement of the CD rings away from the stilbene units shortens the length of the rotaxane **2** and the distance between the blocking groups. Therefore, the isomers *E,E*-, *E,Z*-, and *Z,Z*-**2** represent, respectively, the extended, intermediate, and contracted states of a reversible, light driven molecular mimic of a muscle sarcomere (Fig. 4).

4.3   A Molecular Information Ratchet

As anticipated above, by appropriate design of the axle component it is possible to control both the thermodynamics and the kinetics underlying the ring shuttling motion in a rotaxane, thus mimicking energy ratcheting mechanisms which are the basis of the operation of biomolecular machines [7–9, 72]. An interesting example is represented by compound **3** in Fig. 5a [73]. The system starts at chemical
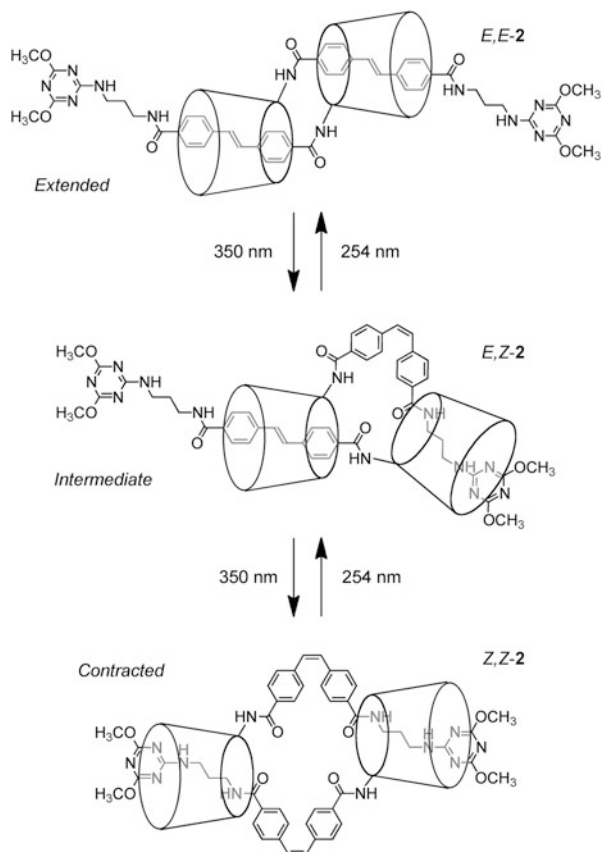
equilibrium, that is, with 85% of macrocycles on the fumaramide station and 15% on the succinamide station, as a consequence of the different affinities of the ring for these two sites (Fig. 5b). Because of the presence of the bulky silyl group R on the axle, ring shuttling in this rotaxane is associated with a large kinetic barrier. When statistical balance is broken by light excitation that causes $E \rightarrow Z$ isomerization of the fumaramide station and the kinetic barrier is removed, the system moves towards the new equilibrium. Restoring the barrier produces a system that is balanced but cannot equilibrate because shuttling is prevented. Hence, the thermal $Z \rightarrow E$ back isomerization makes the system statistically unbalanced and out of equilibrium. In this rotaxane the axle can perform the task of directionally changing the net position of the macrocycle. Eventually, the removal of the bulky substituent allows the system to reach equilibrium and restore the original ring distribution.

The same principle has been exploited to obtain the first example of a molecular information ratchet [74]. The described system is rotaxane 4^{2+} which consists of a dibenzo[24]crown-8-based macrocycle mechanically locked onto a linear molecular axle (Fig. 6). Along the axle there are two stations for the ring − a dibenzylammonium
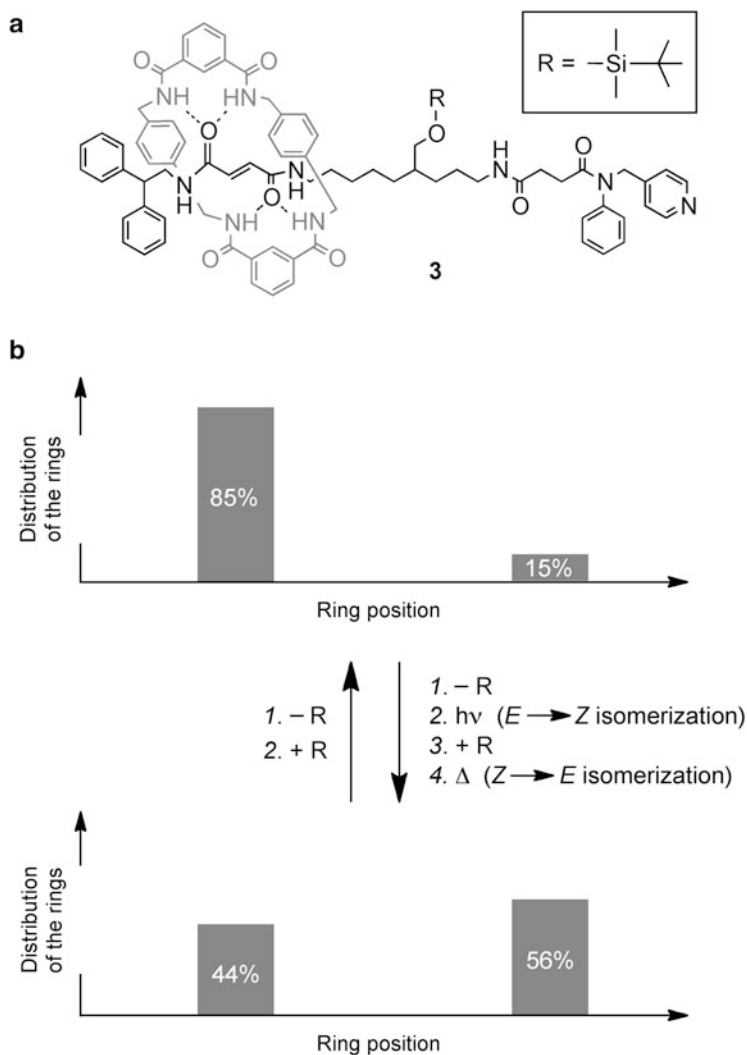
Fig. 5 (**a**) Structural formula of rotaxane 3, in which the ring movement caused by $E{\rightarrow}Z$ photoisomerization is made irreversible by insertion of a barrier after the $E{\rightarrow}Z$ transformation and shuttling. The result is a change in the net position of the macrocycle (**b**)

(DBA$^+$) and a monobenzylammonium (MBA$^+$) unit – which bind the ring with comparable affinities, but are distinguishable for the purpose of monitoring the system. An α-methylstilbene unit divides the axle asymmetrically into two compartments, each containing a station. When the stilbene unit is in the E form, the macrocycle can move randomly along the full length of the axle, whereas when the stilbene unit is in the Z form, the ring is trapped in one of the two compartments. Therefore, the stilbene unit plays the role of a photoswitchable gate for the ring movement between the two
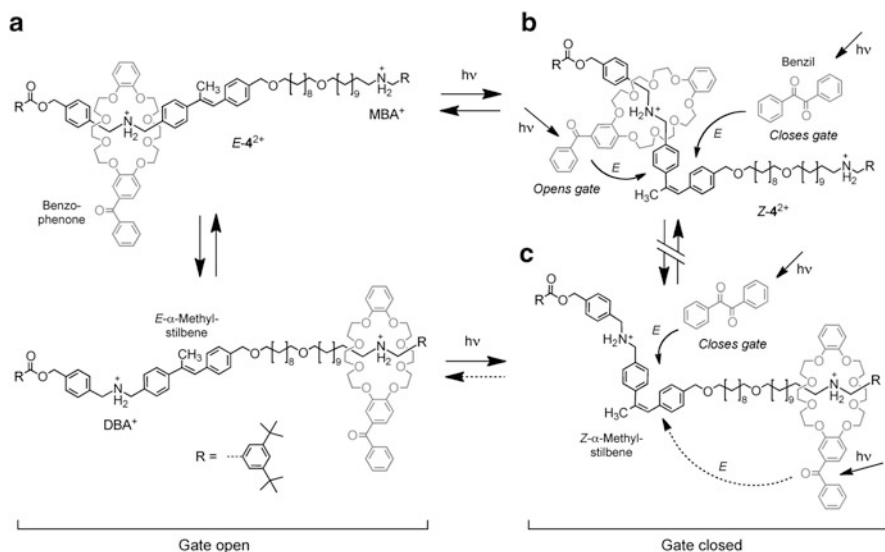
Fig. 6 Scheme for operation of a molecular information ratchet based on the photoisomerizable bistable rotaxane $\mathbf{4}^{2+}$. *Dashed arrows* indicate processes that are unlikely to occur

stations. With the stilbene unit is in the E form (i.e., gate open) an equilibrium distribution of the ring between the two stations of $65(DBA^+):35(MBA^+)$ is established (Fig. 6a).

To drive the ring distribution away from equilibrium, the gate should be closed for most of the time, and opened preferentially when the macrocycle occupies a specific position (in this case the DBA^+ station). The first requirement is obtained by adding to the solution a suitable photosensitizer (benzil) which leads to a photostationary state rich in the *cis* form of α-methylstilbene (82:18 *Z:E* under the conditions employed) by intermolecular triplet sensitization. The second requirement is accomplished by appending another photosensitizer (benzophenone) to the macrocycle, capable of causing the $Z–E$ photoisomerization of the stilbene gate by intramolecular triplet sensitization. Benzophenone was chosen because it leads to a photostationary state more rich in the E form of α-methylstilbene (55:45 $Z:E$) compared to benzil. A key feature of the system is that the DBA^+ station is very close to the stilbene gate, whereas the MBA^+ station is relatively distant from the gate. Therefore, it can be expected that intramolecular (benzophenone) sensitization (i.e., gate opening) is more efficient when the macrocycle is in the DBA^+ compartment, whereas the efficiency of intermolecular (benzil) sensitization should be independent on the location of the macrocycle. Conditions are chosen so that the benzophenone-sensitized isomerization dominates (gate open) when the ring is in the DBA^+ compartment – that is, held near to the gate (Fig. 6b) – whereas the benzil-sensitized reaction dominates (gate closed) when the ring is in the MBA^+ compartment – that is, held far from the gate (Fig. 6c).

27A. Credi et al.

Fig. 7 Schematic representation of an information ratchet mechanism for the directional transport of a Brownian particle along a potential energy surface. If the particle signals its position in a distance-dependent manner, then only the barrier closer to the particle may be lowered
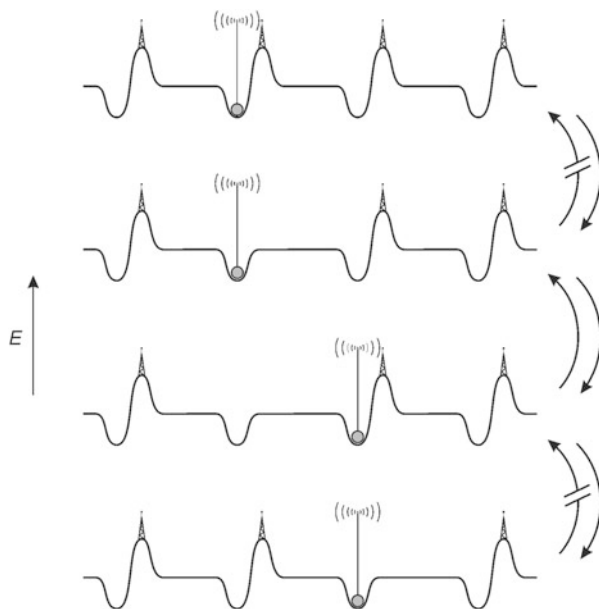
The system starts with the stilbene gate open (E) and an equilibrium ring distribution of 65(DBA$^+$):35(MBA$^+$). Irradiation in the presence of a suitable amount of benzil leads the system to an 80:20 Z:E photostationary state. Under this condition, the ring distribution becomes 45(DBA$^+$):55(MBA$^+$); that is, about one-third of the macrocycles which occupied the more energetically favorable DBA$^+$ compartment at equilibrium have been moved to the less favorable MBA$^+$ compartment. Ultimately, the different photoreactivity of the various interconverting isomers of 4^{2+} (Fig. 6) leads to a ring distribution between the two compartments under light irradiation which is different from that observed at the equilibrium in the dark.

It should be pointed out that in this system photons are not used to modify the binding energy between the ring and either station, but to power an information transfer process, as schematically indicated in Fig. 7 [6]. In other words, driving the ring distribution away from its equilibrium value is ensured only by the fact that the macrocycle "signals" its position to the gate, which opens (or closes) accordingly. The similarity of these processes with the hypothetical task performed without an energy input by a "demon" in Maxwell's famous thought experiment has been extensively discussed [6].
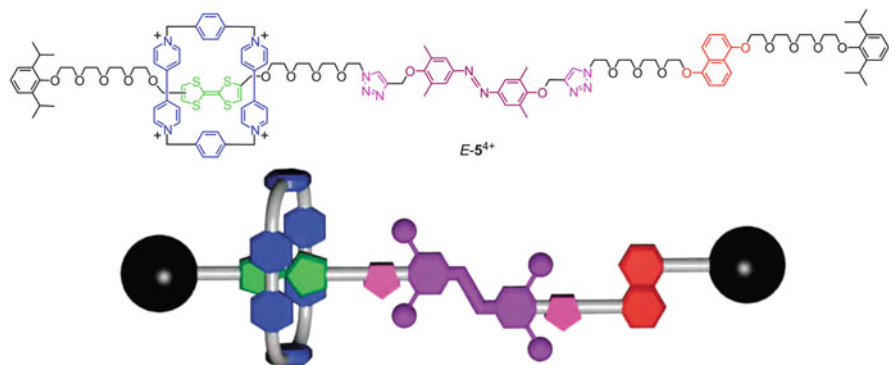
**Fig. 8** Structural formula and schematic representation of rotaxane 5^{4+}

4.4 Light-Induced Memory Effects in a Bistable Molecular Shuttle

Recently, the bistable rotaxane 5^{4+} in which orthogonal chemical and optical stimuli are used to gain full control on the thermodynamics (i.e., the distribution of the rings between the two sites located along the axle) and the kinetics (i.e., the translation rate of the rings between the sites) of molecular shuttling was described (Fig. 8) [75]. A system of this kind is interesting not only from the view point of molecular machines but also from that of signal processing and storage. As a matter of fact, controllable molecular shuttles can be considered as bistable mechanical switches at the nanoscale [76]. While the operation of bistable molecular switches is based on classical switching processes between thermodynamically stable states, the development of molecular memories – which rely on a sequential logic behavior [77] – also requires a control of the rates of the mechanical movement between such states.

The functional units incorporated in the multicomponent rotaxane 5^{4+} (Fig. 8) are: (1) the π-electron-deficient CBPQT^{4+} ring; (2) the π-electron donor recognition sites of the dumbbell component, constituted by a tetrathiafulvalene (TTF) unit and a 1,5-dioxynaphthalene (DNP) unit; and (3) a photoactive 3,5,3′,5′-tetramethylazobenzene (TMeAB) moiety, located in between the TTF and DNP units, which can be reversibly and efficiently switched between its E and Z configurations by photochemical stimuli. Since the TTF unit is more π-electron rich than the DNP one, the CBPQT^{4+} macrocycle prefers to encircle the TTF unit rather than the DNP one in the starting co-conformation of 5^{4+} (Fig. 9). This preference is evidenced by the presence of a charge-transfer (CT) band peaking at 850 nm in its absorption spectrum (Fig. 10). Upon chemical or electrochemical oxidation of the TTF unit to its radical cation (TTF$^{•+}$) form, signaled by the appearance of the TTF$^{•+}$ absorption features in the 400–650 nm region (Fig. 10), CBPQT^{4+} shuttles to the DNP recognition site on account of the electrostatic repulsion caused by the TTF$^{•+}$ radical cation and the loss of π-donor–acceptor interactions with CBPQT^{4+}. Such a
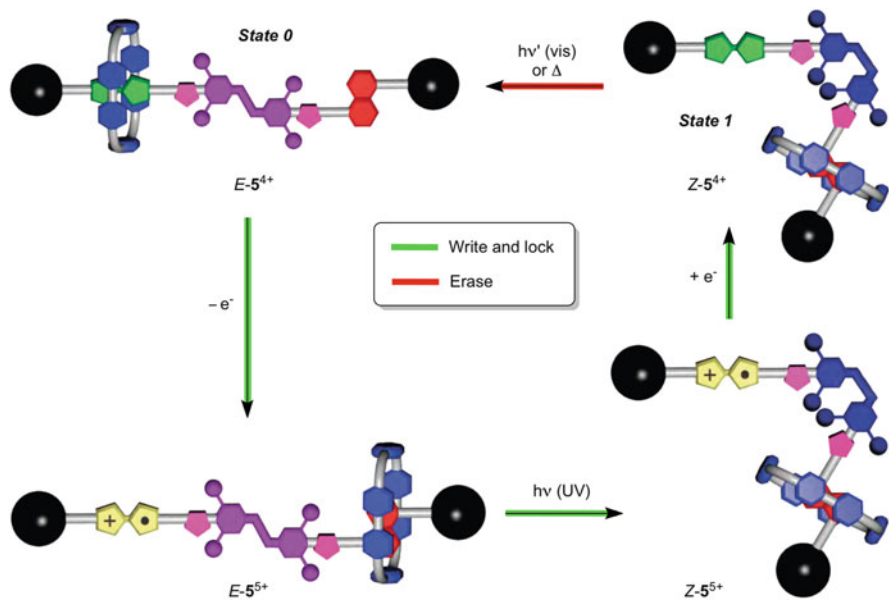
Fig. 9 Chemically and photochemically triggered memory switching cycle of rotaxane 5^{4+}
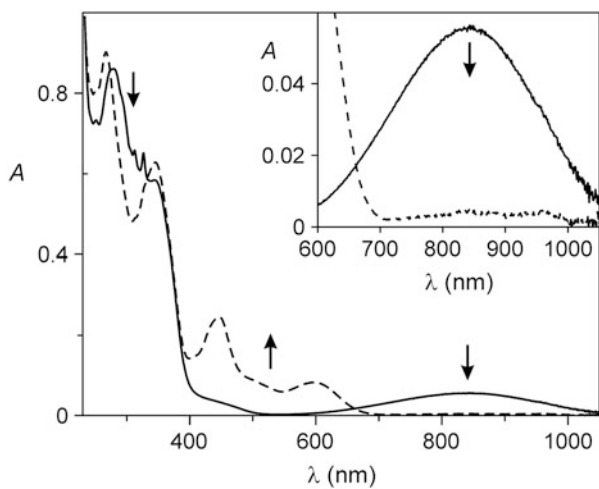
Fig. 10 Absorption spectrum of a 19 μM solution of E-5^{4+} (CH$_3$CN, 295 K) before (*solid curve*) and after (*dashed curve*) oxidation with 1 equiv. of Fe(ClO$_4$)$_3$ to obtain E-5^{5+}

process can be monitored by the disappearance of both the CT band at 850 nm and the sharp absorption features at around 320 nm, typical of the DNP site not surrounded by $CBPQT^{4+}$ (Fig. 10).

Steady-state and time-resolved UV-visible spectroscopic experiments showed that, upon quick chemical reduction of the $TTF^{\bullet+}$ unit to its neutral state, the $CBPQT^{4+}$ ring immediately shuttles back to encircle the TTF site if the TMeAB unit is in the E configuration, whereas it remains trapped on the DNP site if the TMeAB unit has been photoisomerized to the Z isomer prior to the $TTF^{\bullet+} \rightarrow TTF$ back reduction (Fig. 9). Indeed, the first-order rate constant for replacement of the $CBPQT^{4+}$ ring onto the regenerated TTF site in the photoisomerized rotaxane, obtained by monitoring the recovery of the CT absorption band at around 850 nm, is in very good agreement with the first-order rate constant corresponding to the thermal $Z \rightarrow E$ isomerization of the TMeAB unit, measured by observing the recovery of the absorption band of the E-TMeAB unit at 344 nm (Fig. 11). This behavior can be explained considering that the E–Z isomerization of TMeAB brings about a large geometrical change capable of affecting substantially the free-energy barrier for the shuttling of $CBPQT^{4+}$ along the axle component [78]. The azobenzene unit in its Z configuration indeed poses a much greater steric hindrance to the shuttling of the ring than does an E azobenzene unit.

In summary, the switching cycle of rotaxane $\mathbf{5}^{4+}$ (Fig. 9) consists of the following steps: (1) oxidation of TTF, causing the shuttling of $CBPQT^{4+}$ from the $TTF^{\bullet+}$ to the DNP site; (2) UV light irradiation, converting the TMeAB unit from the E to the Z configuration (gate closed); (3) back reduction, regenerating the neutral TTF unit with the $CBPQT^{4+}$ still residing on the DNP unit, and (4) successive photochemical or thermal $Z \rightarrow E$ back isomerization, opening the gate and enabling the replacement of $CBPQT^{4+}$ onto the TTF primary recognition site.

In other words, in a "write-lock-erase" experiment based on the cycle shown in Fig. 9, the data is written on the rotaxane by an oxidation stimulus, and locked by UV light irradiation; after the writing session, the oxidized species can be reduced back to the original form without losing the written data for a remarkably longer time compared to thermodynamically controlled molecular switches. Indeed, the data remain stored for a few hours in the dark at room temperature until the thermal opening of the azobenzene gate occurs. Therefore, $\mathbf{5}^{4+}$ operates as a bistable memory element under light-triggered kinetic control. It is also important to note that light irradiation not only locks the data previously recorded by oxidation but also protects the nonoxidized rotaxanes from accidental writing. These properties have positive implications for the use of such molecules in engineered test devices [79, 80].

Another elegant strategy to affect the shuttling kinetics by using light makes use of an intramolecular photocycloaddition reaction and its thermal reversion to shrink the macrocyclic component of a rotaxane [81].
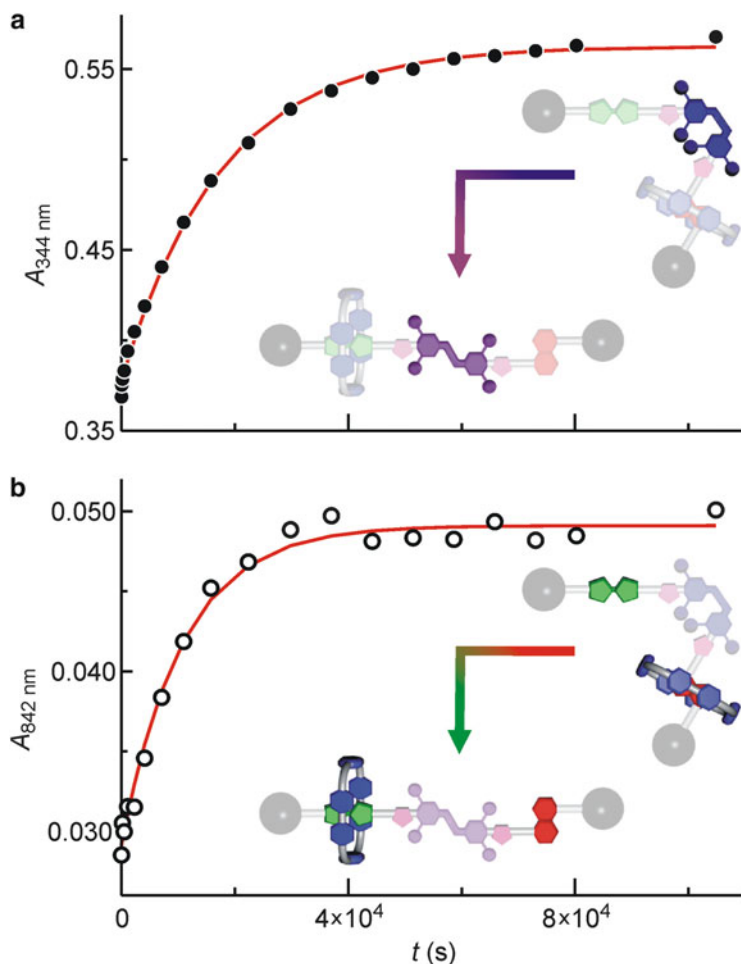
Fig. 11 Time-dependent absorption changes (CH_3CN, 295 K), monitored at (**a**) 344 nm (*E*-TMeAB absorption) and (**b**) 842 nm (TTF-CBPQT^{4+} CT absorption), showing the regeneration of *E*-$\mathbf{5}^{4+}$ from the metastable state *Z*-$\mathbf{5}^{4+}$. The lines represent the data fitting according to a first-order kinetic equation. Adapted with permission from [75]

5   Molecular Threading/Dethreading with Directional Control

The examples discussed in the previous sections demonstrate that the principles and methods of supramolecular chemistry applied to the construction of working devices and molecular machines represent a powerful strategy for the development of nanoscience and nanotechnology as well as for the comprehension of the several biological processes in which natural motors and machines operate [8, 9, 82].
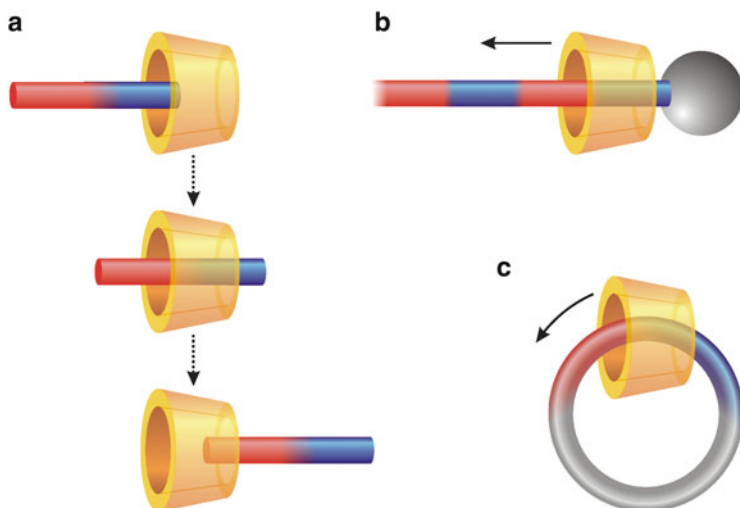
Fig. 12 Representation of unidirectional threading/dethreading of a [2]pseudorotaxane with nonsymmetric components (**a**), a processive linear motor based on a [2]rotaxane (**b**), and a rotary motor based on a [2]catenane (**c**). Reprinted with permission from [102]

Pseudorotaxanes, supramolecular complexes minimally composed of a ring-type host surrounding an axle-type guest [45], are the simplest prototypes of artificial molecular level machines [5]. As already mentioned, their working mechanism is based on the assembly/disassembly of the axle and ring components and it resembles the threading/dethreading of a needle. Studies on switchable pseudorotaxanes, in which these movements can be controlled by external stimulation [5, 46], are of great interest not only for the development of functional materials [83] but also for the realization of molecular machines based on rotaxanes, catenanes, and related interlocked compounds. Specifically, the development of a pseudorotaxane motif capable of performing unidirectional threading and dethreading processes [84–86] under control of external stimuli (Fig. 12a) would be important for the construction of processive linear motors based on rotaxanes (Fig. 12b) and, at least as a perspective, rotary motors based on catenanes (Fig. 12c) [6, 13].

The essential feature of molecular motors is indeed the directional control of the motion, which is achieved by modulating not only the thermodynamics but also the kinetics of the transition between the mechanical states of the device. This result can be achieved by applying ratcheting concepts to the design of the systems [6, 13, 87]. A few examples of artificial molecular rotary motors and DNA-based linear motors [44, 88, 89] have been described, and fully synthetic linear motor molecules are available (see chapters by Leigh and Willner in this volume) [90]. Such systems, however, are based on sophisticated chemical species and/or their operation relies on a complex sequence of chemical reactions. Therefore, the development of concepts and structures for the construction of linear supramolecular motors characterized by simple, efficient and reversible operation is still an open problem and an important challenge, because linear movements are essential both in Nature and technology.
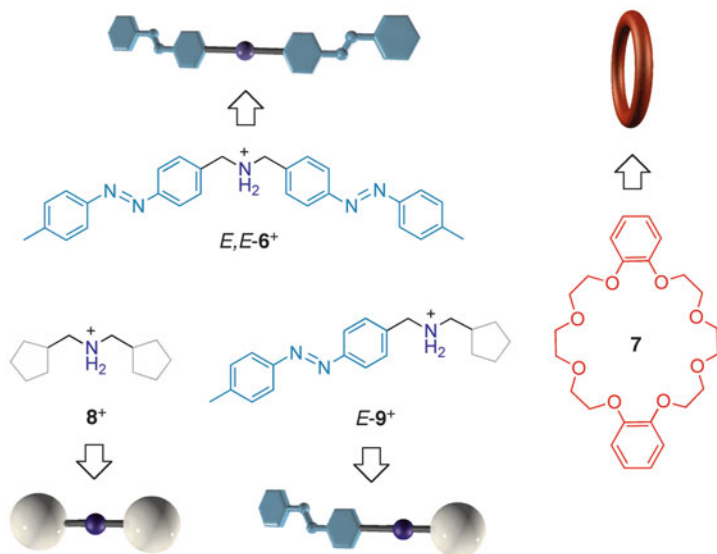
Fig. 13 Structure formulas and schematic representation of the examined axle **6**$^+$ and ring 7

5.1 Photocontrolled Unidirectional Transit of a Molecular Axle Through a Macrocycle

As discussed above, the control of the relative direction of threading and dethreading in pseudorotaxanes cannot be achieved simply by means of classical switching processes between thermodynamically stable states (disassembled components/assembled complex) [13]. The rates of the transition processes between such states also have to be controlled in order to make the desired processes faster than the undesired ones.

A first step forward towards this goal is the ability to adjust the threading/dethreading kinetics by modulating the corresponding energy barriers through external stimulation. A system that can be reversibly photoswitched between thermodynamically stable (pseudorotaxane) and kinetically inert (rotaxane) states is based on the molecular components **6**$^+$ and **7** shown in Fig. 13 [91]. The molecular axle **6**$^+$ comprises a secondary ammonium center as a hydrogen-bonding donor and two photoswitchable azobenzene end groups. In organic solution, **6**$^+$ and the dibenzo[24]crown-8 ring **7** self-assemble to yield a pseudorotaxane complex (Fig. 14), on account of hydrogen bonding between the secondary ammonium center of the axle and the oxygen atoms of the crown ether, with possible contributions from π-stacking interactions between the aromatic moieties of **7** and the azobenzene units. Remarkably, the $E{\rightarrow}Z$ photoisomerization of the azobenzenes at both ends of axle **6**$^+$ slows down the threading/dethreading of ring **7** by at least four orders of magnitude. The threading time constants under the
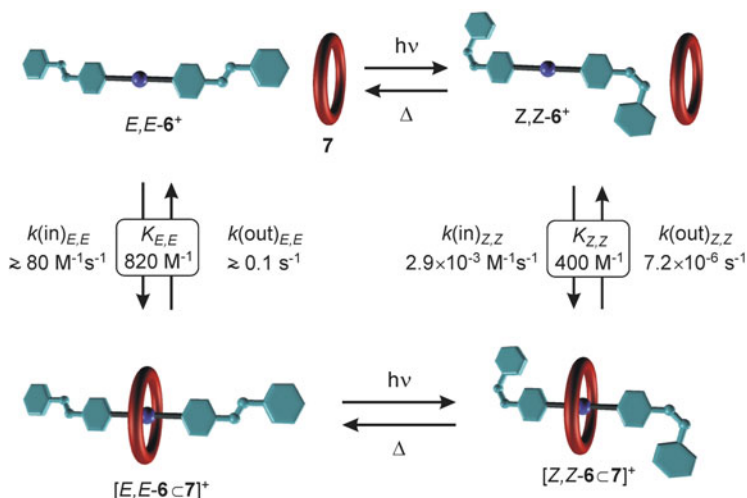
Fig. 14 Operation scheme of a self-assembling system that can be reversibly photoswitched between thermodynamically stable (pseudorotaxane) and kinetically inert (rotaxane) forms

conditions adopted (room temperature, 5 mM acetonitrile solutions) are >2.5 s and 20 h for E,E-6^+ and Z,Z-6^+, respectively. Another interesting feature of this system is that the thermodynamic stability of the complex is also affected by light: the association constant of 6^+ with 7 drops by a factor of two on going from the E,E to the Z,Z isomer of the axle. Moreover, the host–guest recognition can be switched off by deprotonating the ammonium center of 6^+ with a base, i.e., using a stimulus orthogonal to that employed for switching the azobenzene end units [91].

Other rotaxane-type systems in which the threading/dethreading kinetics can be photocontrolled according to strategies similar to that described above have been reported in the recent literature [92, 93].

Building upon the results described above, the operation of a simple supramolecular assembly in which a molecular ring translates unidirectionally along a molecular axle in response to photochemical and chemical stimulation has recently been reported [94]. As discussed in Sect. 3, it should be remembered that in solution only the movements of the ring and axle components relative to one another can be considered; therefore, an equally valid view of the device operation would be to consider that the molecular axle passes through the cavity of the macrocyclic component. In fact, such a convention will be used to describe the systems presented in this and the next sections. Besides the implications for the realization of molecular linear motors based on rotaxanes and rotary motors based on catenanes (Fig. 12), a system of this kind constitutes a first step towards the construction of an artificial molecular pump.

The device (Fig. 15) is based on a non-symmetric axle molecule comprising three different functional units: (1) a passive pseudo-stopper (D), (2) a central ammonium recognition site (S) for the ring, and (3) a photoswitchable azobenzene
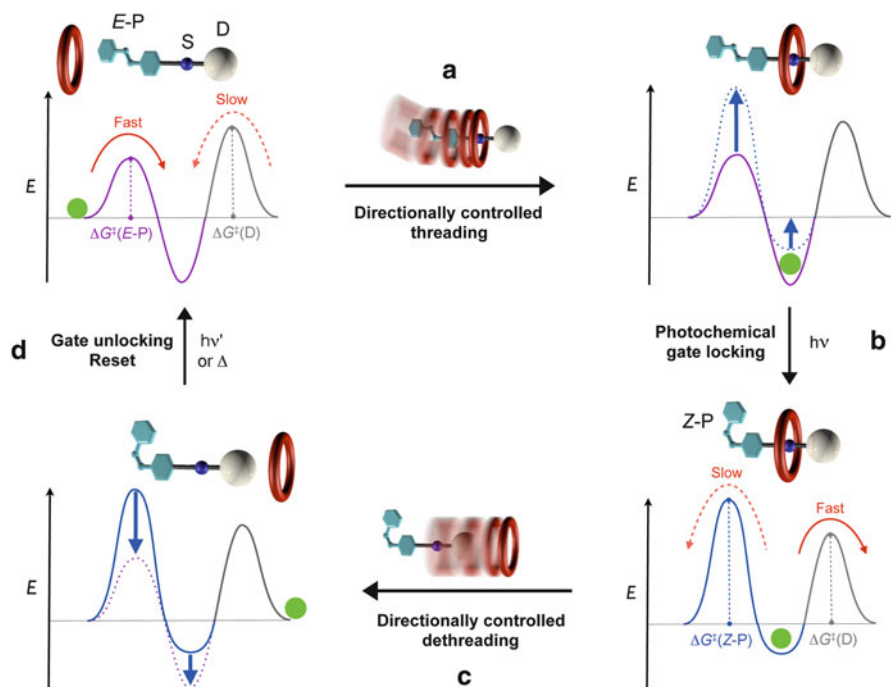
Fig. 15 Strategy for the photoinduced unidirectional transit of a molecular ring along a non-symmetric molecular axle. Simplified potential energy curves (free energy vs ring-axle distance) for the states shown, describing the operation of the system in terms of a flashing ratchet mechanism, are also reported

unit (P) at the other end. As for the system described in Fig. 14, the ring-axle recognition relies primarily on hydrogen-bonding interactions involving the ammonium center of the axle and the crown ether oxygen atoms.

The strategy at the basis of the operation of this ensemble is shown schematically in Fig. 15. In acetonitrile solution, for kinetic reasons, the axle threads the ring exclusively from the side of the photoactive gate in its starting E configuration (Fig. 15a), affording a pseudorotaxane in which the molecular ring encircles the recognition site S. Light irradiation converts the E–P end group into the angular Z form, a process which is also expected to destabilize the supramolecular complex (Fig. 15b) [91]. Therefore, the dethreading of a fraction of the axle molecules in the pseudorotaxane population is expected, which occurs by exit of the axles from the side carrying the D moiety (Fig. 15c). The system is brought back to its initial state by photochemical or thermal conversion of the Z–P gate back to the E configuration (Fig. 15d). Overall, the photoinduced directionally controlled transit of the axle through the ring would be obtained according to a flashing energy ratchet mechanism [6, 72].

There are two basic requirements for this strategy to work: (1) the kinetic barriers for the slippage of the ring through the axle end groups should follow the

$\Delta G^{\ddagger}(E\text{–P}) < \Delta G^{\ddagger}(\text{D}) < \Delta G^{\ddagger}(Z\text{–P})$ order, and (2) the ring should form a more stable pseudorotaxane when the axle has the photoswitchable end group in its E configuration compared to the Z one. It is also important that the differences in the kinetic and stability constants are sufficiently large, and that the photochemical interconversion of the P gate between its E and Z forms is fast, efficient, and reversible.

It is clear that the choice of the pseudo-stopper unit D is crucial for the successful operation of the mechanism shown in Fig. 15. It was previously reported [95] that the bis(cyclopentylmethyl)ammonium ion 8^+ (Fig. 13) is complexed by 7 to form a pseudorotaxane, with threading and dethreading rate constants that fall nicely in between those observed for $E,E\text{-}6^+$ and $Z,Z\text{-}6^+$ with the same ring [91]. Hence, the strategy shown in Fig. 14 can be implemented with the non-symmetric axle $E\text{-}9^+$, derived from the symmetric guests $E,E\text{-}6^+$ and 8^+ (Fig. 13).

^{1}H NMR spectroscopic titration experiments showed that in acetonitrile $E\text{-}9^+$ pierces ring 7 exclusively from the E-azobenzene terminus. Irradiation of $E\text{-}9^+$ with UV light affords $Z\text{-}9^+$ in an almost quantitative way. The increased hindrance of the azobenzene end group upon photoisomerization forces $Z\text{-}9^+$ to thread 7 through its cyclopentyl terminus. It should be noted that the $E{\rightarrow}Z$ photoisomerization of the azobenzene end group of 9^+ also takes place efficiently when it is surrounded by 7. Therefore kinetic control of the threading/dethreading side of 9^+ can be achieved by photoadjusting the steric hindrance of its azobenzene end group.

In contrast with the results found for the $[E,E\text{-}6{\subset}7]^+$ and $[Z,Z\text{-}6{\subset}7]^+$ pseudorotaxanes [91], the stability constants of $[E\text{-}9{\subset}7]^+$ and $[Z\text{-}9{\subset}7]^+$ are identical within errors. Therefore, in acetonitrile the dethreading of $Z\text{-}9^+$ from the ring cannot be caused by the same photochemical stimulus that triggers the azobenzene $E{\rightarrow}Z$ isomerization. Because deprotonation of the ammonium recognition site of $Z\text{-}9^+$ with a base causes the fast dethreading from 7, thereby neutralizing the stoppering ability of the Z-azobenzene unit, K^+ ions were used as competitive guests for 7 [96] in order to promote the disassembly of the complexes. The addition of 2 equiv. of KPF_6 causes the complete dethreading of both $[E\text{-}9{\subset}7]^+$ and $[Z\text{-}9{\subset}7]^+$; however, while at room temperature the K^+-induced disassembly of the former complex is immediate, the latter one exhibits a dethreading half-life of 51 min (Fig. 16). Considering that the K^+-induced dethreading of $[Z,Z\text{-}6{\subset}7]^+$ occurs with a half-life of ca. 40 h (Fig. 16) [91], these observations indicate that the chemically induced disassembly of $Z\text{-}9^+$ from 7 takes place exclusively by slippage of the ring through the cyclopentyl end of the axle.

The results of an experiment that illustrates the directional transit of the ring along the axle are summarized in Fig. 17: (1) $E\text{-}9^+$ pierces 7 with its E-azobenzene side to form the pseudorotaxane $[E\text{-}9{\subset}7]^+$; (2) irradiation in the near UV region converts quantitatively $[E\text{-}9{\subset}7]^+$ into $[Z\text{-}9{\subset}7]^+$, characterized by slow assembly-disassembly kinetics; (3) the successive addition of K^+ ions promotes the dethreading of $Z\text{-}9^+$ from 7 by the passage of the cyclopentyl moiety through the cavity of the ring. It should be noted that equilibration of the $[Z\text{-}9{\subset}7]^+$ complex with its separated components, that would cause the loss of the information on the threading direction of $E\text{-}9^+$, is much slower than the time required for the activation
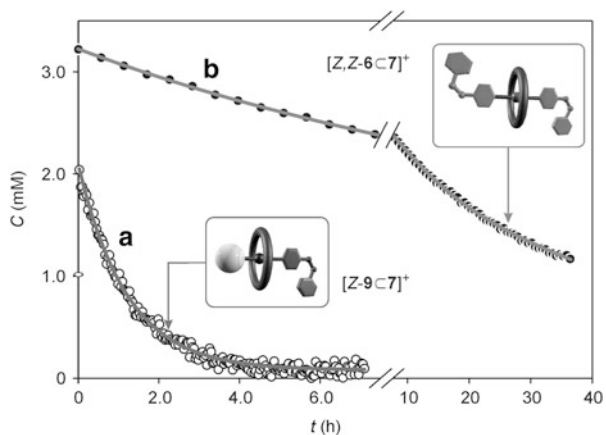
Fig. 16 Time-dependent concentration changes, obtained from ^{1}H NMR data in CD$_3$CN at 298 K, showing the K$^+$-induced dethreading of (**a**) [Z-9⊂7]$^+$ and (**b**) [Z,Z-6⊂7]$^+$. Conditions: (**a**) 5.1 mM Z-9H$^+$, 5.4 mM 7 (about 40% complexation of the axle molecules), 15.2 mM KPF$_6$; (**b**) 4.8 mM Z, Z-6H$^+$, 7.6 mM 7 (about 65% complexation of the axle molecules), 16.7 mM KPF$_6$. Reprinted with permission from [94]
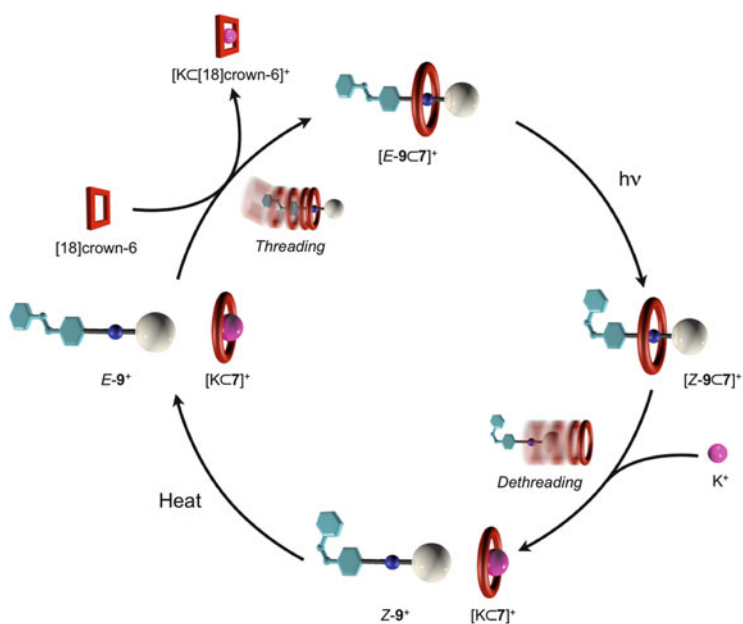
**Fig. 17** Representation of the photochemically and chemically controlled transit of 7 along **9$^+$**

of the dethreading stimulus (addition of K^+). Therefore, after the threading event the system is "locked" by photoisomerization, and the successive addition of potassium ions causes dethreading in the same direction along which threading of E-9^+ has initially occurred. The starting species E-9^+ can be fully regenerated by thermal $Z \rightarrow E$ back isomerization, and sequestration of K^+ by an excess of [18] crown-6 affords the re-assembly of $[E$-$9 \subset 7]^+$ and the full reset of the system.

This supramolecular system, however, if it were to be incorporated in a compartmentalized structure (e.g., embedded in the membrane of a vesicle), could not be used to "pump" the molecular axle and generate a transmembrane chemical potential because the ring component has two identical faces. Despite this deficiency the described system is characterized by a minimalist design, facile synthesis, convenient switching, and reversibility: all these features constitute essential requirements for real world applications.

In the next section a strategy similar to that just described is applied to supramolecular assemblies based on three-dimensional non-symmetric macro-cycles whose lengths can approach the thickness of a bilayer membrane, [97] and in which face-selective threading can be realized.

5.2 Solvent- and Light-Controlled Unidirectional Transit of a Non-symmetric Molecular Axle through a Non-symmetric Three-Dimensional Macrocycle

An increase in the structural complexity of the self-assembled pseudorotaxane/rotaxane systems can be obtained by using as a ring component the macrocycle tris (phenylureido)calix[6]arene [98] derivative **10** (Fig. 18). Because of the non-symmetric nature of this "wheel" it is possible to thread selectively suitable axles from the "upper" or "lower" rim of the macrocycle leading to "up" and "down" oriented isomers (Fig. 19). It is known [99] that, in apolar media, macrocycle **10** is able to be threaded exclusively from the upper rim by axles derived from 4,4′-bipyridinium salts [100]. This behavior can be explained by the peculiar chemical and structural features of compound **10** as a host, which are (1) a π-donor cavity that, because of its width, can include the positively charged bipyridinium unit of the axle, but not together with its counter anions, (2) three efficient hydrogen-bonding donor ureidic groups at the upper rim that, by complexing the counter anions of the axle, can assist the insertion of the cationic portion of the latter, and (3) three methoxy groups at the lower rim that, in apolar media, are oriented towards the interior of the cavity [101], thereby hindering the access of the guest from this direction. The use of more polar solvents has a profound effect on these interactions. In fact, the solvent polarity, by changing the extent of ion pairing of the axle and decreasing the pivoting role of the three ureidic groups of the host, affects both the concentration of the active guest available in solution and the binding ability of the macrocycle.
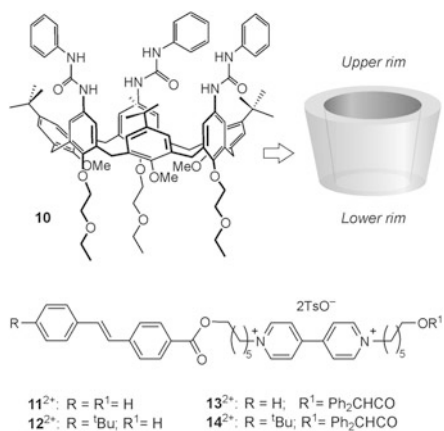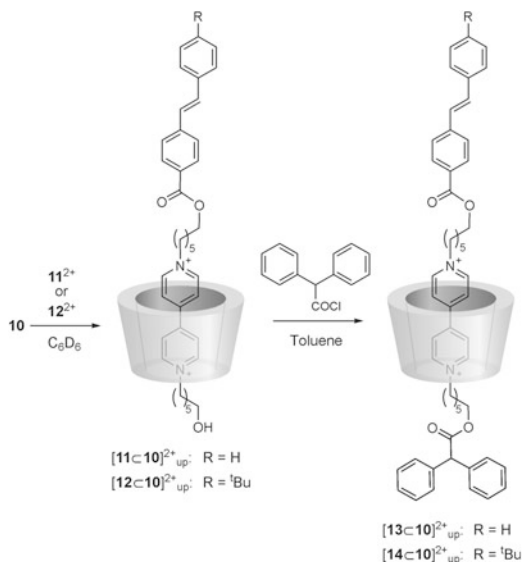
Fig. 18 Structural formulas of the examined ring and axle components
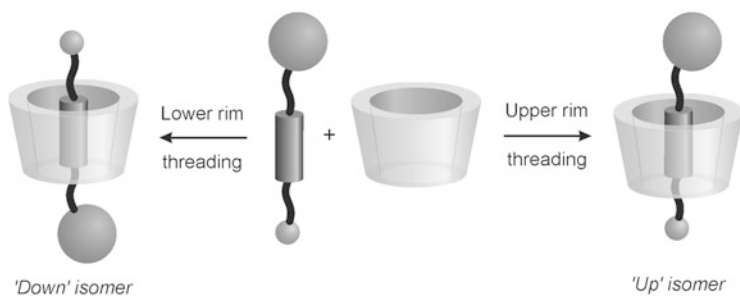
Fig. 19 Formation of "up" and "down" oriented pseudorotaxane isomers by self-assembly of the nonsymmetric ring and axle components

To obtain pseudorotaxane systems based on ring **10**, capable of undergoing relative unidirectional threading/dethreading motion, the axles **11**$^{2+}$ and **12**$^{2+}$ (Fig. 18) were employed [102]. They are composed of a central electron-acceptor 4,4′-bipyridinium unit functionalized with a hexanol chain on one side and either a stilbene (**11**$^{2+}$) or a ^{t}Bu-substituted stilbene (**12**$^{2+}$) on the other. The terminal OH group has been selected because it can be involved in stoppering reactions, while the stilbene and the ^{t}Bu-substituted stilbene head groups have been employed because they are not too bulky to prevent their slippage [103, 104] through **10**, but large enough to enable a kinetic control of the threading/dethreading motions of the ring. NMR spectra of the equilibrium mixture obtained after mixing **10** with an excess of axle **11**$^{2+}$ or **12**$^{2+}$ in C$_6$D$_6$ at room temperature prove that only one pseudorotaxane type complex forms predominantly, confirming that both axles enter the calixarene cavity through the calixarene upper rim with their OH terminus to yield the oriented species [**11**⊂**10**]$^{2+}_{up}$ and [**12**⊂**10**]$^{2+}_{up}$ (Fig. 20). This orientational control during the formation of the pseudorotaxane indicates

Fig. 20 Self-assembly of pseudorotaxanes $[11 \subset 10]^{2+}_{up}$ and $[12 \subset 10]^{2+}_{up}$, and synthesis of semirotaxanes $[13 \subset 10]^{2+}_{up}$ and $[14 \subset 10]^{2+}_{up}$

$[11 \subset 10]^{2+}_{up}$: R = H
$[12 \subset 10]^{2+}_{up}$: R = ^{t}Bu

$[13 \subset 10]^{2+}_{up}$: R = H
$[14 \subset 10]^{2+}_{up}$: R = ^{t}Bu

that the macrocycle promotes the threading of the axles from the upper rim and that the latter components access the macrocycle through the less bulkier OH terminus in a process that is kinetically controlled by the different size of the end groups of the axles. When the OH end group of pseudorotaxanes $[11 \subset 10]^{2+}_{up}$ and $[12 \subset 10]^{2+}_{up}$ is replaced by bulky diphenylacetyl moieties, the pseudorotaxanes are converted to semirotaxanes $[13 \subset 10]^{2+}_{up}$ and $[14 \subset 10]^{2+}_{up}$ (Fig. 20). These species exhibit a more pronounced rotaxane-like behavior than $[11 \subset 10]^{2+}_{up}$ and $[12 \subset 10]^{2+}_{up}$ because one end of their axle is stoppered by the presence of the bulky diphenylacetyl moiety, while dethreading from the side carrying the stilbene-type unit is greatly slowed down by the steric hindrance of the latter.

In polar solvents the multiple interactions that stabilize complexes $[13 \subset 10]^{2+}_{up}$ and $[14 \subset 10]^{2+}_{up}$ are weakened and, therefore, dissolution of these species in such solvents induces the dethreading of the axle. Because of the presence of the diphenylacetyl stopper at one end of the axles, the dethreading occurs through the slippage of the sufficiently slim stilbene-type unit from the calixarene lower rim. The dethreading rate in DMSO for semirotaxane $[13 \subset 10]^{2+}_{up}$ (Fig. 21a) is two orders of magnitude lower than that of $[14 \subset 10]^{2+}_{up}$, owing to the higher hampering effect of the ^{t}Bu-substituted stilbene present in axle 14^{2+} compared with the unsubstituted axle 13^{2+}.

In these semirotaxanes the dethreading rate can also be photocontrolled upon UV light-induced E–Z isomerization of the stilbene end group of the axles. For both $[13 \subset 10]^{2+}_{up}$ and $[14 \subset 10]^{2+}_{up}$ at the photostationary state about 70% of the stilbene units are converted from the E to the Z isomer. In the case of $[13 \subset 10]^{2+}_{up}$ the higher hampering effect of the Z isomer compared with the E one results in a much more difficult slippage of this unit through the lower rim of the macrocycle once it is dissolved in a polar solvent (Fig. 21b). It is interesting to notice that the E–Z

Fig. 21 Time-dependent
absorption changes at
460 nm observed upon
dissolution of $[13 \subset 10]^{2+}_{up}$
in DMSO at room
temperature, before
(**a**, *full circles*) and after
(**b**, *open circles*) exhaustive
irradiation at 334 nm,
causing the $E \rightarrow Z$
isomerization of the stilbene
end group. The first-order
fitting curves are also shown
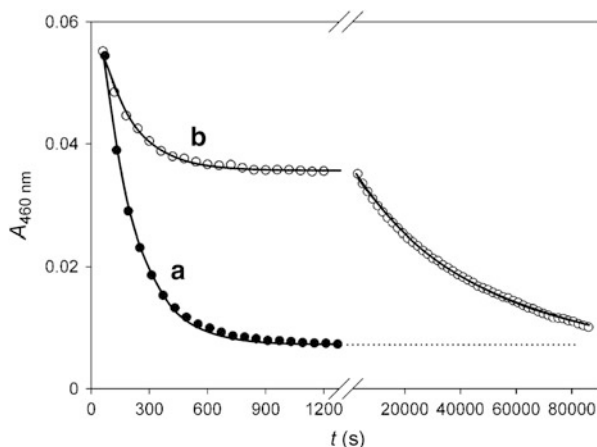
photoisomerization affects the dethreading rate constant to a greater extent than
does the incorporation of the ^tBu group on the stilbene unit. The rate constant
observed upon isomerization is indeed about one order of magnitude slower than
that observed for the E-isomer of the substituted stilbene.

Remarkably, in the case of $[14 \subset 10]^{2+}_{up}$ the photoisomerized compound does not
undergo dethreading in polar solvents at all. The Z isomer of the ^tBu-stilbene is too
bulky to pass through the calixarene lower rim, and $[14 \subset 10]^{2+}_{up}$ in its
Z configuration exhibits a genuine rotaxane behavior.

According to the transformation sequence described above, and as schematized
in Fig. 22, the unidirectional transit of the non-symmetric molecular axles 11^{2+} and
12^{2+} through the non-symmetric macrocycle **10** (or the translation of the ring along
the axles) is achieved. The strategy is based on the use of appropriately designed
molecular components, an essential feature of which is their nonsymmetric
structure, and exploits the following steps: (1) in apolar solvents axles 11^{2+} or
12^{2+} thread calixarene **10** from its upper rim, leading to an oriented pseudorotaxane
structure in which the OH group is positioned at the lower rim of the ring; this
threading mode is favored because of the small hampering effect of the OH group
being substantially lower than that of the stilbene moiety (Fig. 22a); (2) by a
stoppering reaction that introduces a bulky diphenylacetyl moiety, the
pseudorotaxane is converted into a semirotaxane-like species (Fig. 22b); and
(3) replacement of the apolar solvent with a polar one weakens the interactions
that stabilize the assembled structure and induces the axle dethreading from the
calixarene lower rim (Fig. 22c), that is, in the same direction of the axle threading.

It is also important to stress the essential role played by the stilbene unit
incorporated at one end of the axle. It enables one: (1) to achieve the unidirectional
transit of the axle through the macrocycle, because its dimensions are not too large
to prevent slippage, but big enough to induce a kinetic control of the axle threading/
dethreading processes; and (2) to tune the dethreading rate because of the
possibility of modifying its hindering effect upon the use of stilbene unit substituted
with relatively bulky groups, or, more interesting, upon photoisomerization.
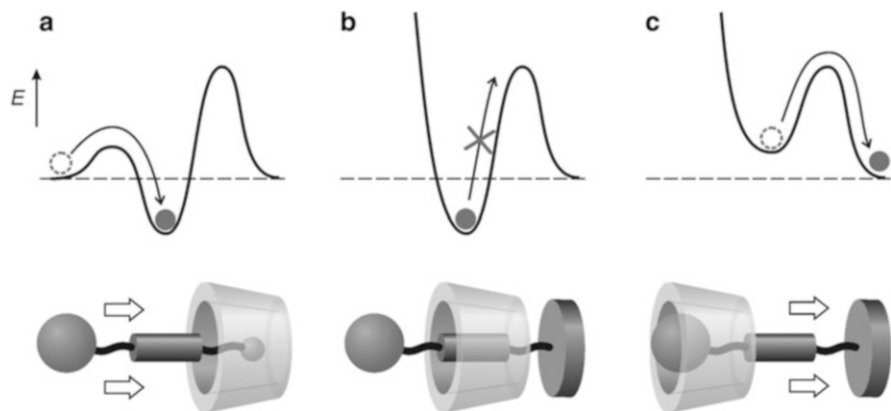
Fig. 22 Simplified potential energy curves representing the relative unidirectional transit of the axle through the ring. The horizontal coordinate of the diagrams represents the axle–ring distance when they approach one another along the direction and with the orientation shown in the drawings. (**a**) Threading of the axle through the macrocycle upper rim in apolar solvents. (**b**) The stoppering reaction that converts the pseudorotaxanes into rotaxane-like species. (**c**) Dethreading of the axle from the macrocycle lower rim in polar solvents

6 Conclusions

One of the most interesting aspects of supramolecular (multicomponent) systems is their interaction with light. The systems described in this chapter show that, in the frame of research on supramolecular photochemistry, the design and construction of nanoscale machines capable of performing useful light-induced functions can indeed be pursued. Their potential applications are various – from energy conversion to sensing and catalysis – and, to a large extent, still unpredictable. As research in the area is progressing, non-conventional functionalities that could be enabled by these systems are emerging. For example, (1) their behavior can be exploited for processing information at the molecular level, and (2) their mechanical features can be utilized for transportation of nanoobjects, mechanical gating of molecular-level channels, and nanorobotics.

It should be noted, however, that the species described here, as most multicomponent systems developed so far, operate in solution, that is, in an incoherent fashion and without control of spatial positioning. Although the solution studies are of fundamental importance to understanding their operation mechanisms and for several uses (e.g., intelligent sensing, catalysis, drug delivery), it seems reasonable that before such systems can find applications in some fields of technology, they have to be interfaced with the macroscopic world by ordering them in some way. The next generation of multicomponent molecular species will need to be organized so that they can behave coherently and can be addressed in space. Viable possibilities include deposition on surfaces, incorporation into polymers, organization at interfaces, or immobilization into membranes or porous materials. Recent achievements in this

direction [18, 69, 70, 105–108] let one be optimistic that useful devices based on functional supramolecular systems could be obtained in a not too distant future.

Apart from foreseeable applications related to the development of nanotechnology, investigations on photochemical molecular machines are important to increase the basic understanding of photoinduced reactions and other important processes such as self-assembly, as well as to develop reliable theoretical models, for example to interpret energy- and electron-transfer processes in complex systems.

It is also important to point out that machines capable of performing useful light-induced functions are of the highest importance in current times. It has become clear that products and services in the years ahead, including those of a nanotechnology-based industry, will have to exploit solar energy [109].

Finally, this research also has the merit of stimulating the ingenuity of chemists, thereby instilling new life into chemistry as a scientific discipline.

References

1. Hader D-P, Tevini M (1987) General photobiology. Pergamon, Oxford
2. Nalwa HS (ed) (2003) Handbook of photochemistry and photobiology, vols 1–4. American Scientific Publishers, Stevenson Ranch
3. Lehn J-M (1988) Supramolecular chemistry – scope and perspectives molecules, supermolecules, and molecular devices (Nobel Lecture). Angew Chem Int Ed Engl 27:89
4. Balzani V (ed) (1987) Supramolecular photochemistry. Reidel, Dordrecht
5. Balzani V, Credi A, Venturi M (2008) Molecular devices and machines – concepts and perspectives for the nanoworld. Wiley-VCH, Weinheim
6. Kay ER, Leigh DA, Zerbetto F (2007) Synthetic molecular motors and mechanical machines. Angew Chem Int Ed 46:72
7. Schliwa M (ed) (2003) Molecular motors. Wiley-VCH, Weinheim
8. Goodsell DS (2004) Bionanotechnology – lessons from nature. Wiley, Hoboken
9. Jones RAL (2005) Soft machines – nanotechnology and life. Oxford University Press, Oxford
10. Shinkai S, Nakaji T, Ogawa T, Shigematsu K, Manabe O (1981) Photoresponsive crown ethers. 2. Photocontrol of ion extraction and ion transport by a bis(crown ether) with a butterfly-like motion. J Am Chem Soc 103:111
11. Kai H, Nara S, Kinbara K, Aida T (2008) Toward long-distance mechanical communication: studies on a ternary complex interconnected by a bridging rotary module. J Am Chem Soc 130:6725
12. Ballardini R, Balzani V, Gandolfi MT, Prodi L, Venturi M, Philp D, Ricketts HG, Stoddart JF (1993) A photochemically driven molecular machine. Angew Chem Int Ed Engl 32:1301
13. Browne WR, Feringa BL (2006) Making molecular machines work. Nat Nanotech 1:25
14. Champin B, Mobian P, Sauvage J-P (2007) Transition metal complexes as molecular machine prototypes. Chem Soc Rev 36:358
15. Balzani V, Credi A, Venturi M (2009) Light powered molecular machines. Chem Soc Rev 38:1542
16. Silvi S, Venturi M, Credi A (2009) Artificial molecular shuttles: from concepts to devices. J Mater Chem 19:2279
17. Ma X, Tian H (2010) Bright functional rotaxanes. Chem Soc Rev 39:70
18. Coskun A, Banaszak M, Astumian RD, Stoddart JF, Grzybowski BA (2012) Great expectations: can artificial molecular machines deliver on their promise? Chem Soc Rev 41:19

19. Balzani V, Credi A, Venturi M (2008) Processing energy and signals by molecular and supramolecular systems. Chem Eur J 14:26
20. Feynman RP (1960) There's plenty of room at the bottom. Eng Sci 23:22
21. Steed JW, Gale PA (eds) (2012) Supramolecular chemistry: from molecules to nanomaterials. Wiley, Chichester, UK
22. Schalley CA (ed) (2012) Analytical methods in supramolecular chemistry, 2nd edn. Wiley-VCH, Weinheim, Germany
23. Balzani V (2003) Photochemical molecular devices. Photochem Photobiol Sci 2:459
24. Marcaccio M, Paolucci F, Roffia S (2004) Supramolecular electrochemistry of coordination compounds and molecular devices. In: Pombeiro AJL, Amatore C (eds) Trends in molecular electrochemistry. Dekker, New York
25. Lakowicz JR (2006) Principles of fluorescence spectroscopy, 3rd edn. Springer, New York
26. Armaroli N, Balzani V (2007) The future of energy supply: challenges and opportunities. Angew Chem Int Ed 46:52
27. Steinberg-Yfrach G, Rigaud J-L, Durantini EN, Moore AL, Gust D, Moore TA (1998) Light-driven production of ATP catalysed by F0F1-ATP synthase in an artificial photosynthetic membrane. Nature 392:479
28. Tian Y, He Y, Chen Y, Yin P, Mao CD (2005) A DNAzyme that walks processively and autonomously along a one-dimensional track. Angew Chem Int Ed 44:4355
29. Muscat RA, Bath J, Turberfield AJ (2011) A programmable molecular robot. Nano Lett 11:982
30. Balzani V, Credi A, Raymo FM, Stoddart JF (2000) Artificial molecular machines. Angew Chem Int Ed 39:3348
31. Stoddart JF (ed) (2001) Acc Chem Res 34(6): special issue on molecular machines
32. Sauvage J-P (ed) (2001) Struct Bond 99: special volume on molecular machines and motors
33. Flood AH, Ramirez RJA, Deng WQ, Muller RP, Goddard WA, Stoddart JF (2004) Meccano on the nanoscale – a blueprint for making some of the world's tiniest machines. Aust J Chem 57:301
34. Kelly TR (ed) (2005) Top Curr Chem 262: special volume on molecular machines
35. Sauvage J-P (2005) Transition metal-complexed catenanes and rotaxanes as molecular machine prototypes. Chem Commun 1507
36. Kottas GS, Clarke LI, Horinek D, Michl J (2005) Artificial molecular rotors. Chem Rev 105:1281
37. Kinbara K, Aida T (2005) Toward intelligent molecular machines: directed motions of biological and artificial molecules and assemblies. Chem Rev 105:1377
38. Tian H, Wang Q-C (2006) Recent progress on switchable rotaxanes. Chem Soc Rev 35:361
39. Willner I (ed) (2006) Org Biomol Chem 4(18); special issue on DNA-based nanoarchitectures and nanomachines
40. Credi A (2006) Artificial molecular motors powered by light. Aust J Chem 59:157
41. Credi A, Tian H (eds) (2007) Adv Funct Mater 17(5): special issue on molecular machines and switches
42. Mateo-Alonso A, Guldi DM, Paolucci F, Prato M (2007) Fullerenes: multitask components in molecular machinery. Angew Chem Int Ed 46:8120
43. Simmel FC, Dittmer WU (2005) DNA nanodevices. Small 1:284
44. Bath J, Turberfield AJ (2007) DNA nanomachines. Nat Nanotechnol 2:275
45. Sauvage J-P, Dietrich-Buchecker C (eds) (1999) Catenanes, rotaxanes and knots. Wiley-VCH, Weinheim
46. Balzani V, Credi A, Venturi M (2002) Controlled disassembling of self-assembling systems: toward artificial molecular-level devices and machines. Proc Natl Acad Sci U S A 99:4814
47. Thordarson P, Nolte RJM, Rowan AE (2004) Mimicking the motion of life: catalytically active rotaxanes as processive enzyme mimics. Aust J Chem 57:323
48. Anelli PL, Spencer N, Stoddart JF (1991) A molecular shuttle. J Am Chem Soc 113:5131

49. Bissell RA, Córdova E, Kaifer AE, Stoddart JF (1994) A chemically and electrochemically switchable molecular shuttle. Nature 369:133
50. Ashton PR, Ballardini R, Balzani V, Credi A, Dress R, Ishow E, Kleverlaan CJ, Kocian O, Preece JA, Spencer N, Stoddart JF, Venturi M, Wenger S (2000) A photochemically driven molecular-level abacus. Chem Eur J 6:3558
51. Balzani V, Clemente-León M, Credi A, Ferrer B, Venturi V, Flood AH, Stoddart JF (2006) Autonomous artificial nanomotor powered by sunlight. Proc Natl Acad Sci U S A 103:1178
52. Brouwer AM, Frochot C, Gatti FG, Leigh DA, Mottier L, Paolucci F, Roffia S, Wurpel GWH (2001) Photoinduction of fast, reversible translational motion in a hydrogen-bonded molecular shuttle. Science 291:2124
53. Panman MR, Bodis P, Shaw DJ, Bakker BH, Newton AC, Kay ER, Brouwer AM, Buma WJ, Leigh DA, Woutersen S (2010) Operation mechanism of a molecular machine revealed using time-resolved vibrational spectroscopy. Science 328:1255
54. Willner I, Pardo-Yissar V, Katz E, Ranjit KT (2001) A photoactivated 'molecular train' for optoelectronic applications: light-stimulated translocation of a beta-cyclodextrin receptor within a stoppered azobenzone-alkyl chain supramolecular monolayer assembly on a Au-electrode. J Electroanal Chem 497:172
55. Stanier CA, Alderman SJ, Claridge TDW, Anderson HL (2002) Unidirectional photoinduced shuttling in a rotaxane with a symmetric stilbene dumbbell. Angew Chem Int Ed 41:1769
56. Qu D-H, Wang Q-C, Ma X, Tian H (2005) A [3]rotaxane with three stable states that responds to multiple-inputs and displays dual fluorescence addresses. Chem Eur J 11:5929
57. Murakami H, Kawabuchi A, Matsumoto R, Ido T, Nakashima N (2005) A multi-mode-driven molecular shuttle: photochemically and thermally reactive azobenzene rotaxanes. J Am Chem Soc 127:15891
58. Dawson RE, Maniam S, Lincoln SF, Easton CJ (2008) Synthesis of alpha-cyclodextrin [2]-rotaxanes using chlorotriazine capping reagents. Org Biomol Chem 6:1814
59. Qu D-H, Wang Q-C, Tian H (2005) A half adder based on a photochemically driven [2] rotaxane. Angew Chem Int Ed 44:5296
60. Li H, Fahrenbach AC, Coskun A, Zhu Z, Barin G, Zhao Y-L, Botros YY, Sauvage J-P, Stoddart JF (2011) A light-stimulated molecular switch driven by radical–radical interactions in water. Angew Chem Int Ed 50:6782
61. Balzani V, Clemente-León M, Credi A, Semeraro M, Venturi M, Tseng H-R, Wenger S, Saha S, Stoddart JF (2006) A comparison of shuttling mechanisms in two constitutionally isomeric bistable rotaxane-based sunlight-powered nanomotors. Aust J Chem 59:193
62. Davidson GJE, Loeb SJ, Passaniti P, Silvi S, Credi A (2006) Wire-type ruthenium (II) complexes with terpyridine-containing [2]rotaxanes as ligands: synthesis, characterization, and photophysical properties. Chem Eur J 12:3233
63. Kosower EM, Cotter JL (1964) Stable free radicals. II. the reduction of 1-methyl-4-cyanopyridinium ion to methylviologen cation radical. J Am Chem Soc 86:5524
64. Watanabe T, Honda K (1982) Measurement of the extinction coefficient of the methyl viologen cation radical and the efficiency of its formation by semiconductor photocatalysis. J Phys Chem 86:2617
65. Champin B, Mobian P, Sauvage J-P (2007) Transition metal complexes as molecular machine prototypes. Chem Soc Rev 36:358
66. Ashton PR, Ballardini R, Balzani V, Baxter I, Credi A, Fyfe MCT, Gandolfi MT, Gomez-Lopez M, Martinez-Diaz M-V, Piersanti A, Spencer N, Stoddart JF, Venturi M, White AJP, Williams DJ (1998) Acid–base controllable molecular shuttles. J Am Chem Soc 120:11932
67. Jiménez MC, Dietrich-Buchecker C, Sauvage J-P (2000) Towards synthetic molecular muscles: contraction and stretching of a linear rotaxane dimer. Angew Chem Int Ed 39:3284
68. Wu J, Leung KC-F, Benitez D, Han J-Y, Cantrill SJ, Fang L, Stoddart JF (2008) An acid-base-controllable [c2]daisy chain. Angew Chem Int Ed 47:7470

69. Fang L, Hmadeh M, Wu J, Olson MA, Spruell JM, Trabolsi A, Yang Y-W, Elhabiri M, Albrecht-Gary A-M, Stoddart JF (2009) Acid–base actuation of [c2]daisy chains. J Am Chem Soc 131:7126

70. Du G, Moulin E, Jouault N, Buhler E, Giuseppone N (2012) Muscle-like supramolecular polymers: integrated motion from thousands of molecular machines. Angew Chem Int Ed 51:12504

71. Dawson RE, Lincoln SF, Easton CJ (2008) The foundation of a light driven molecular muscle based on stilbene and alpha-cyclodextrin. Chem Commun 3980

72. Astumian RD (2007) Design principles for Brownian molecular machines: how to swim in molasses and walk in a hurricane. PhysChemChemPhys 9:5067

73. Chatterjee MN, Kay ER, Leigh DA (2006) Beyond switches: ratcheting a particle energetically uphill with a compartmentalized molecular machine. J Am Chem Soc 128:4058

74. Serreli V, Lee C-F, Kay ER, Leigh DA (2007) A molecular information ratchet. Nature 445:523

75. Avellini T, Li H, Coskun A, Barin G, Trabolsi A, Basuray AN, Dey SK, Credi A, Silvi S, Stoddart JF, Venturi M (2012) Photoinduced memory effect in a redox controllable bistable mechanical molecular switch. Angew Chem Int Ed 51:1611

76. Balzani V, Credi A, Venturi M (2003) Molecular logic circuits. ChemPhysChem 3:49

77. Credi A (2007) Molecules that make decisions. Angew Chem Int Ed 46:5472

78. Coskun A, Friedman DC, Li H, Patel K, Khatib HA, Stoddart JF (2009) A light-gated STOP−GO molecular shuttle. J Am Chem Soc 131:2493

79. Liu Y, Flood AH, Bonvallett PA, Vignon SA, Northrop BH, Tseng H-R, Jeppesen JO, Huang TJ, Brough B, Baller M, Magonov S, Solares SD, Goddard WA, Ho CM, Stoddart JF (2005) Linear artificial molecular muscles. J Am Chem Soc 127:9745

80. van der Molen SJ, Liljeroth P (2010) Charge transport through molecular switches. J Phys Condens Matter 22:133001

81. Hirose K, Shiba Y, Ishibashi K, Doi Y, Tobe Y (2008) A shuttling molecular machine with reversible brake function. Chem Eur J 14:3427

82. Mann S (2008) Life as a nanoscale phenomenon. Angew Chem Int Ed 47:5306

83. Saha S, Leung KCF, Nguyen TD, Stoddart JF, Zink JI (2007) Nanovalves. Adv Funct Mater 17:685

84. Park JW, Song HJ, Cho YJ, Park KK (2007) Thermodynamics and kinetics of formation of orientationally isomeric [2]pseudorotaxanes between α-cyclodextrin and aliphatic chain-linked aromatic donor-viologen acceptor compounds. J Phys Chem C 111:18605

85. Mourtzis N, Eliadou K, Yannakopoulou K (2004) Influence of host's substitution on the orientation of the guest: pseudo-rotaxanes of charged cyclodextrins with methyl orange in solution. Supramol Chem 16:587

86. Oshikiri T, Yamaguchi H, Takashima Y, Harada A (2009) Face selective translation of a cyclodextrin ring along an axle. Chem Commun 5515

87. Kelly TR, de Silva H, Silva RA (1999) Unidirectional rotary motion in a molecular system. Nature 401:150

88. Sherman WB, Seeman NC (2004) A precisely controlled DNA biped walking device. Nano Lett 4:120

89. Simmel FC (2009) Processive motion of bipedal DNA walkers. ChemPhysChem 10:2593

90. von Delius M, Geertsema EM, Leigh DA (2010) A synthetic small molecule that can walk down a track. Nat Chem 2:96

91. Baroncini M, Silvi S, Venturi M, Credi A (2010) Reversible photoswitching of rotaxane character and interplay of thermodynamic stability and kinetic lability in a self-assembling ring–axle molecular system. Chem Eur J 16:11580

92. Tokunaga Y, Akasaka K, Hashimoto N, Yamanaka S, Hisada K, Shimomura Y, Kakuchi S (2009) Using photoresponsive end-closing and end-opening reactions for the synthesis and disassembly of [2]rotaxanes: implications for dynamic covalent chemistry. J Org Chem 74:2374

93. Ogoshi T, Yamafuji D, Aoki T, Yamagishi T (2011) Photoreversible transformation between seconds and hours time-scales: threading of pillar[5]arene onto the azobenzene-end of a viologen derivative. J Org Chem 76:9497

94. Baroncini M, Silvi S, Venturi M, Credi A (2012) Photoactivated directionally controlled transit of a non-symmetric molecular axle through a macrocycle. Angew Chem Int Ed 51:4223

95. Ashton PR, Campbell PJ, Chrystal EJT, Glink PT, Menzer S, Philp D, Spencer N, Stoddart JF, Tasker PA, Williams DJ (1995) Dialkylammonium ion/crown ether complexes: the forerunners of a new family of interlocked molecules. Angew Chem Int Ed 34:1865

96. Takeda Y, Kudo Y, Fujiwara S (1985) Thermodynamic study for complexation reactions of dibenzo-24-crown-8 with alkali metal ions in acetonitrile. Bull Chem Soc Jpn 58:1315

97. Arduini A, Credi A, Faimani G, Massera C, Pochini A, Secchi A, Semeraro M, Silvi S, Ugozzoli F (2008) Self-assembly of a double calix[6]arene pseudorotaxane in oriented channels. Chem Eur J 14:98

98. Arduini A, Bussolati R, Credi A, Faimani G, Garaudee S, Pochini A, Secchi A, Semeraro M, Silvi S, Venturi M (2009) Towards controlling the threading direction of a calix[6]arene wheel by using nonsymmetric axles. Chem Eur J 15:3230

99. Credi A, Dumas S, Silvi S, Venturi M, Arduini A, Pochini A, Secchi A (2004) Viologen-calix [6]arene pseudorotaxanes. Ion-pair recognition and threading/dethreading molecular motions. J Org Chem 69:5881

100. Arduini A, Ciesa F, Fragassi M, Pochini A, Secchi A (2005) Selective synthesis of two constitutionally isomeric oriented calix[6]arene-based rotaxanes. Angew Chem Int Ed 44:278

101. van Duynhoven JPM, Janssen RG, Verboom W, Franken SM, Casnati A, Pochini A, Ungaro R, De Mendoza J, Nieto PM, Prados P, Reinhoudt DN (1994) Control of calix[6] arene conformations by self-inclusion of 1,3,5-tri-O-alkyl substituents: synthesis and NMR studies. J Am Chem Soc 116:5814

102. Arduini A, Bussolati R, Credi A, Monaco S, Secchi A, Silvi S, Venturi M (2012) Solvent- and light-controlled unidirectional transit of a nonsymmetric molecular axle through a nonsymmetric molecular wheel. Chem Eur J 18:16203

103. Ashton PR, Baxter I, Fyfe MCT, Raymo FM, Spencer N, Stoddart JF, White AJP, Williams DJ (1998) Rotaxane or pseudorotaxane? That is the question! J Am Chem Soc 120:2297

104. Affeld A, Hubner GM, Seel C, Schalley CA (2001) Rotaxane or pseudorotaxane? Effects of small structural variations on the deslipping kinetics of rotaxanes with stopper groups of intermediate size. Eur J Org Chem 15:2877

105. Berna J, Leigh DA, Lubomska M, Mendoza SM, Perez EM, Rudolf P, Teobaldi G, Zerbetto F (2005) Macroscopic transport by synthetic molecular machines. Nat Mater 4:704

106. Green JE, Choi JW, Boukai A, Bunimovich Y, Johnston-Halperin E, DeIonno E, Luo Y, Sheriff BA, Xu K, Shin YS, Tseng HR, Stoddart JF, Heath JR (2007) A 160-kilobit molecular electronic memory patterned at 10(11) bits per square centimetre. Nature 445:414

107. Wang C, Li ZX, Cao D, Zhao YL, Gaines JW, Bozdemir OA, Ambrogio MW, Frasconi M, Botros YY, Zink JI, Stoddart JF (2012) Stimulated release of size-selected cargos in succession from mesoporous silica nanoparticles. Angew Chem Int Ed 51:5460

108. Kudernac T, Ruangsupapichat N, Parschau M, Macia B, Katsonis N, Harutyunyan SR, Ernst KH, Feringa BL (2011) Electrically driven directional motion of a four-wheeled molecule on a metal surface. Nature 479:208

109. Ceroni P, Credi A, Venturi M, Balzani V (2010) Light-powered molecular devices and machines. Photochem Photobiol Sci 9:1561